Optik 162 (2018) 214–219

Contents lists available at ScienceDirect

Optik

journal homepage: www.elsevier.de/ijleo

Low-loss polarization filter at 1.55 μm based on photonic crystal fiber

Chao Dou[a,b], Xili Jing[a,*], Shuguang Li[a], Junjun Wu[a,c], Qingbo Wang[a,d]

[a] State Key Laboratory of Metastable Materials Science & Technology and Key Laboratory for Microstructural Material Physics of Hebei Province, School of Science, Yanshan University, Qinhuangdao, 066004, PR China
[b] Department of Basic Education, Tangshan University, Tangshan 063000, PR China
[c] College of Qing Gong, North China University of Science and Technology, Tangshan 063009, PR China
[d] Department of Physics, Tangshan Normal University, Tangshan 063000, PR China

ARTICLE INFO

Article history:
Received 29 November 2017
Received in revised form 6 February 2018
Accepted 14 February 2018

Keywords:
Polarization filter
Photonic crystal fiber
Surface plasmon resonance

ABSTRACT

In this paper, a photonic crystal fiber with the gold layer is simulated by finite element method. Due to birefringence, surface plasmon resonance only occurs in the y-polarization direction. The loss of y-polarization mode is much larger than that of x-polarization mode. The photonic crystal fiber is suitable for the polarization filter. The polarization filter has the short length and high extinction ratio. Furthermore, the insertion loss of the x-polarization mode is only 0.07 dB, which is the smallest as far as we know.

© 2018 Elsevier GmbH. All rights reserved.

1. Introduction

Photonic crystal fibers (PCFs) [1] are usually based on silica as a background material, with the periodic arrangement of pores along the axial direction. The size of the pores is approximately the same as the wavelength of the light, so PCFs are also known as holey fibers (HFs) or microstructure optical fibers (MOFs). The structure of PCF is flexible, and the arrangement of the pores can greatly affect the transfer characteristics. The transfer characteristics also can be changed by selectively filling or coating different materials into the pores, such as semiconductor material [2], liquid crystal [3] or metal [4].

When the light transmits in a photonic crystal fiber with metal layer, the free electrons in the metal will absorb the energy of the light wave, forming surface plasmon polaritons (SPPs). The light wave can couple with SPPs, and surface plasmon resonance (SPR) occurs when their phases match [5]. Zhang et al. have firstly demonstrated that selective metal coating in the PCFs is feasible [6]. Nagasaki et al. have investigated the position of the metal wires has a significant influence on the transmission characteristics of the PCFs [7]. Heikal et al. have proposed a novel selectively metal-filled spiral photonic crystal fiber for filters [8]. Sun et al. have proposed a polarization splitter with the bandwidth as great as 146 nm, by the inclusion of metal wire in PCF [9]. Li et al. have verified the operating wavelengths of optical polarizer based on the gold-filled PCF can be modulated by adjusting the wire size [10]. Khaleque et al. have proposed a compact gold-filled dualcore PCF, which is a candidate for the polarization splitter, having a short length of 117 μm [11]. With the development of plasma technology, SPR has been widely applied in optical device.

* Corresponding author.
E-mail address: sljingxl@ysu.edu.cn (X. Jing).

https://doi.org/10.1016/j.ijleo.2018.02.044
0030-4026/© 2018 Elsevier GmbH. All rights reserved.

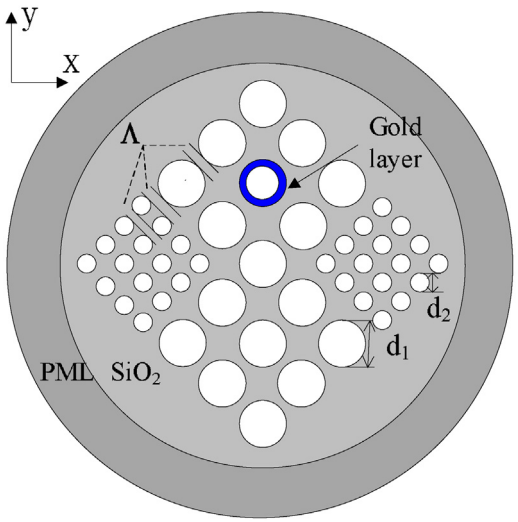

Fig. 1. Cross section of PCF with the gold layer.

In this paper, we propose a single-polarization PCF with a square lattice. The PCF is simulated by finite element method. The gold layer is coated on a pore sited in the y-direction. Due to surface plasmon resonance, the confinement loss of y-polarization mode is much larger than that of x-polarization mode. A PCF suitable for the polarization filter can be obtained.

2. Structure of PCF

The cross section of the proposed PCF is shown in Fig. 1. The background material of the fiber is pure silica, whose dispersion relationship is calculated by the Sellmeier equation [12]. The PCF consists of two sizes of pores, forming a square-lattice. The diameter of the big pores (denoted by d_1) is 1.9 μm, and the diameter of the small pores (denoted by d_2) is 0.9 μm. The spacing between the edges of adjacent holes (denoted by Λ) is 0.1 μm. This arrangement can maintain the stability of the PCF structure and reduce the difficulty of fiber drawing. A pore sited in the y direction is coated with gold layer. The thickness of gold layer (denoted by t) is 32 nm. The permittivity of the gold layer is calculated by the Drude-Lorentz model [13].

The asymmetric structure make the PCF have high birefringence. When the light is transmitted in a high birefringence PCF, the light can be separated into two orthogonal polarized modes. Due to having the different refractive index, propagation velocity and phase, the two polarization modes are separated. Thus the PCFs with high birefringence can be utilized to fabricate the optical polarization devices.

3. Simulations and discussions

The simulation software is Comsol Multiphysics, and the finite element method (FEM) is utilized to calculate the characteristics of the PCF. The scattering boundary conditions and perfect matched layer are employed in the simulation process, and the thickness of perfect matched layer is assumed to be 3 μm.

Fig. 2 shows the effective index curves of the four modes: x-polarization core mode (x-PCM), y-polarization core mode (y-PCM), x-surface plasmon polaritons mode (x-SPPM) and y-surface plasmon polaritons mode (y-SPPM). As the wavelength increases, the effective index of the four modes decreases. The dispersion curves of x-PCM and x-SPPM have no intersection in the whole waveband. However the dispersion curves of y-PCM and y-SPPM intersect at the wavelength of 1.55 μm. At the intersection point, the two modes meet the phase matching conditions, and the surface plasmon resonance (SPR) is stimulated in the y direction [7].

The confinement loss spectra is shown in Fig. 3. The loss of x-PCM exhibits a straight line parallel to the x-axis, varies little with wavelength. The loss of x-SPPM is far greater than the loss of x-PCM. The two curves do not intersect in the whole wavelength range. Hence there is no resonance between x-PCM and x-SPPM. At 1.55 μm, the loss of x-PCM is only 1.5 dB/cm. By contrast, two curves of y-PCM and y-SPPM intersect at 1.55 μm, where the loss of y-PCM appears a peak and the loss of y-SPPM appears a valley. It indicates the energy is transferred from y-PCM to y-SPPM. At 1.55 μm, the loss of y-PCM is 1005.5 dB/cm. The intensity of SPR reaches its maximum, the formant corresponds to the intersection point in Fig. 2.

Fig. 4a and b shows the mode field distributions of x-PCM and y-PCM when no coupling occurs. All the energy is concentrated in the central region of the mode field. Fig. 4c shows the mode field distribution of y-SPRM. Part of the energy is concentrated in the center of the mode field, and the other part of the energy is distributed on the surface of gold layer. At the wavelength of 1.55 μm, the energy is maximally transferred from y-PCM to y-SPPM, which is called complete coupling.

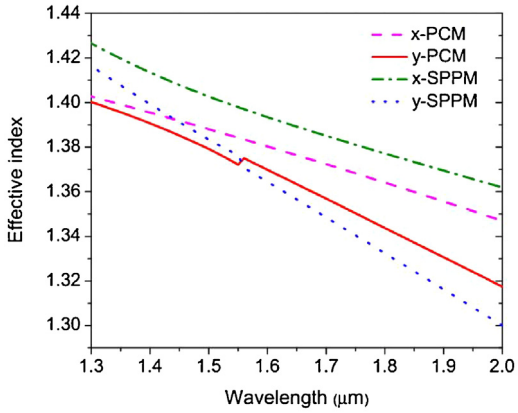

Fig. 2. Dispersion relations of core modes and SPP modes.

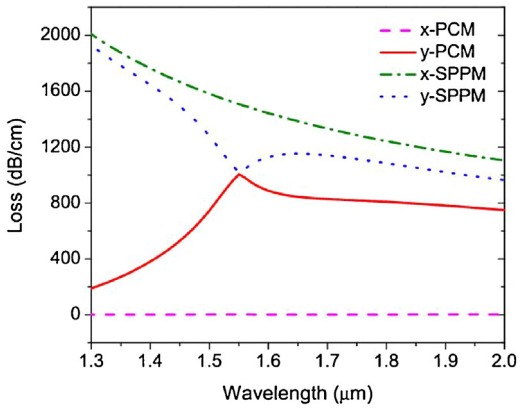

Fig. 3. Confinement loss varies along with the wavelength.

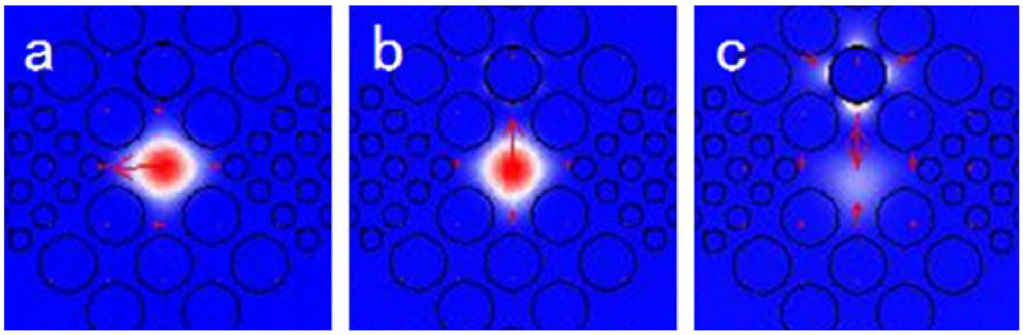

Fig. 4. Distributions of the electric field of (a) x-PCM (b) y-PCM (c) y-SPRM.

When the input power is considered to 1, the normalized output power can be obtained by the equation [14]:

$$P_{out}(x, y) = \exp(-\alpha(x, y) \times L \times \frac{\ln 10}{10}) \quad (1)$$

L represents fiber length.

Assume that the fiber length is 0.25, 0.5 and 1 mm, respectively. Fig. 5 shows the normalized output power of x- and y-polarization mode, which is represented by Px and Py. As the wavelength increases, Px decreases slightly in the whole wavelength range, Py first decreases rapidly and then maintains a stable value. Comparing the curves of different fiber lengths, it can be seen that the increasement of the fiber length has a weak impact on Px, but has a significant impact on Py. Table 1 shows the comparison of Px and Py at 1.55 μm of different fiber lengths. When the fiber length is 0.5 mm, Px and Py

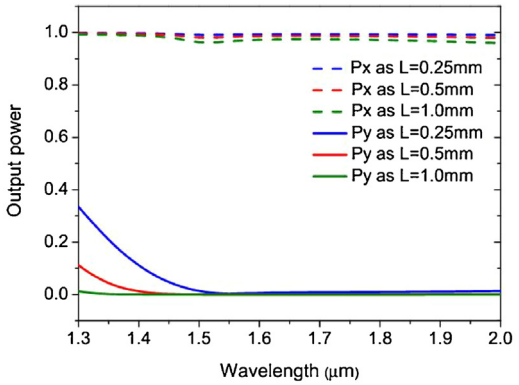

Fig. 5. Normalized output power varies along with the wavelength.

Table 1
Comparison of the normalized output power.

	L = 0.25 mm	L = 0.5 mm	L = 1.0 mm
Px	0.991	0.983	0.966
Py	0.003	9.39×10^{-6}	8.81×10^{-11}

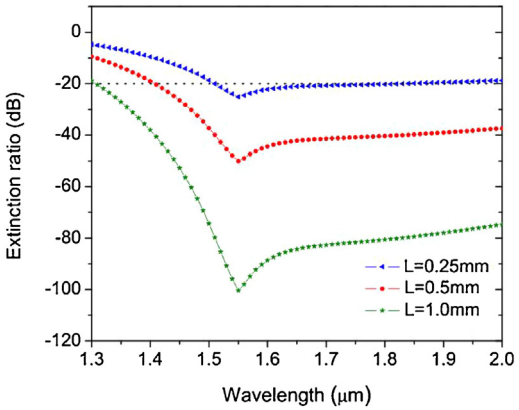

Fig. 6. Extinction ratios of PCF filter with different fiber length.

Table 2
Comparison of extinction ratios.

	L = 0.5 mm	L = 2 mm	L = 3 mm	L = 4 mm
Ref. [16]		118.7dB	−178.0dB	−273.3dB
Our design	−50.2dB	−200.8dB	−301.2dB	−401.6dB

are 0.98 and 9.39×10^{-6}. It indicates the transmission of x-polarization mode is permitted in the PCF, but the transmission of y-polarization mode is suppressed. Our proposed PCF is suitable for manufacturing single polarization filters.

The performance of the polarization filter can be evaluated by extinction ratio (*ER*), which is calculated by the following equation [15]:

$$ER = 10\log_{10}\left(\frac{P_{out}(y)}{P_{out}(x)}\right) \tag{2}$$

where P_{out} is the output power, P_{in} is the input power.

The extinction ratio (ER) is an important parameter for the polarization filter. When ER is less than -20 dB, the ratio of Px and Py is greater than 100, the y-polarization mode disappears in the emergent light [15]. Fig. 6 depicts the ER curves of the PCF polarization filter. When the length of the polarization filter is 0.25, 0.5, 1.0 mm, the maximal value reaches −25.1, −50.2, −100.4 dB, which appears at 1.55 μm. In Fig. 6, the bandwidth with ER less than −20 dB is from 1.51 to 1.82 μm, 1.41 to 2.0 μm, 1.31 to 2.0 μm, respectively. Tables 2 and 3 show the parameters comparison between our polarization filter and

Table 3
Comparison of bandwidth.

	L = 0.5 mm	L = 2 mm	L = 3 mm	L = 4 mm
Ref. [16]		1.19–1.7 μm	1.48–1.86 μm	1.48–2.0 μm
Our design	1.41–2.0 μm	1.22–2.0 μm	1.17–2.0 μm	1.13–2.0 μm

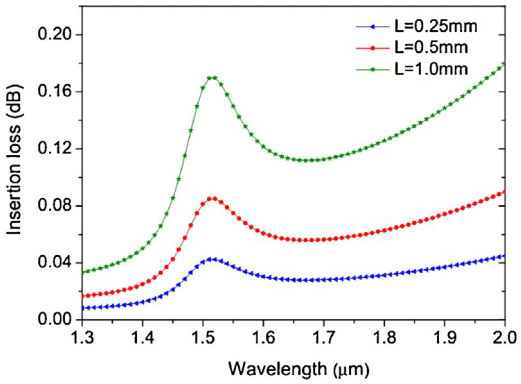

Fig. 7. Insertion loss of the PCF filter with different fiber lengths.

Table 4
Comparison of insertion loss.

	Insertion loss (dB)	Fiber length (mm)
Ref. [16]	7.382	2.0
Ref. [17]	0.135	0.5
Our design	0.070	0.5

reference [16]. By comparison, when two filters have the same length, our filter has smaller ER than the filter proposed in reference [16], and the bandwidth with ER less than −20 dB is much wider.

The insertion loss (*IL*) is also a problem that must be considered when designing an optical communication device, which is defined as [15]:

$$IL = -10\log_{10}\left(\frac{P_{out}}{P_{in}}\right) \tag{3}$$

P_{in} and P_{out} is the power of polarized light, when we calculate *IL* of the polarization filter.

Fig. 7 shows that the insertion loss is proportional to the fiber length. When the length is 0.25, 0.5 and 1.0 mm, IL at 1.55 μm is only 0.035, 0.07 and 0.15 dB, and the maximum value of IL is 0.045, 0.09 and 0.18 dB, respectively. In the entire wavelength range, the insertion loss is small enough to satisfy the optical transmission requirement.

In summary, both the extinction ratio and insertion loss are proportional to the fiber length. When the extinction ratio is -50 dB, the ratio of the output power of two polarization modes is as high as 100,000. The two polarization modes can be divided very well. Thus the excessive extinction ratio has no practical application significance, but will increase the insertion loss. Considering the extinction ratio and insertion loss comprehensively, we set the length of our filter to 0.5 mm, whose ER is −50.2 dB and the insertion loss is only 0.07 dB.

In the existing literatures, most polarization filters aimed to improve the extinction ratio, but ignored the discussion of insertion loss. In Table 4, we add the insertion loss of the polarization filters, which are not discussed in reference [16] and [17]. By contrast, the insertion loss of our filter is only half of that in reference [17], and far less than that in reference [16]. To the best of our knowledge, the insertion loss of our filter is the smallest.

Finally, the error tolerances in the actual production are analyzed. Fig. 8a shows that when the scaling ratio of the fiber cross section is 90% and 110%, ER at 1.55 μm is −47.7 and −32.9 dB. The bandwidth with ER less than −20 dB is from 1.34 to 2.0 μm and from 1.48 to 2.0 μm. Fig. 8b shows that when the variations of the thickness of gold layer is −10% and 10%, ER at 1.55 μm is −43.8 and −43.1 dB. The bandwidth with ER less than −20 dB is from 1.43 to 2.0 μm and from 1.40 to 2.0 μm. The data shows that when the error tolerance is controlled within ±10%, the filter still has a good performance.

4. Conclusion

In this paper, a PCF for making the polarization filter is proposed. SPR only is excited in the y-polarization direction. As a result, the loss of y-polarization mode at 1.55 μm is 1005.5 dB/cm while the loss of x-polarization mode is just 1.5 dB/cm. We can obtain a single polarization filter, whose normalized output power of x and y-polarization mode is 0.98 and 9.39×10^{-6}.

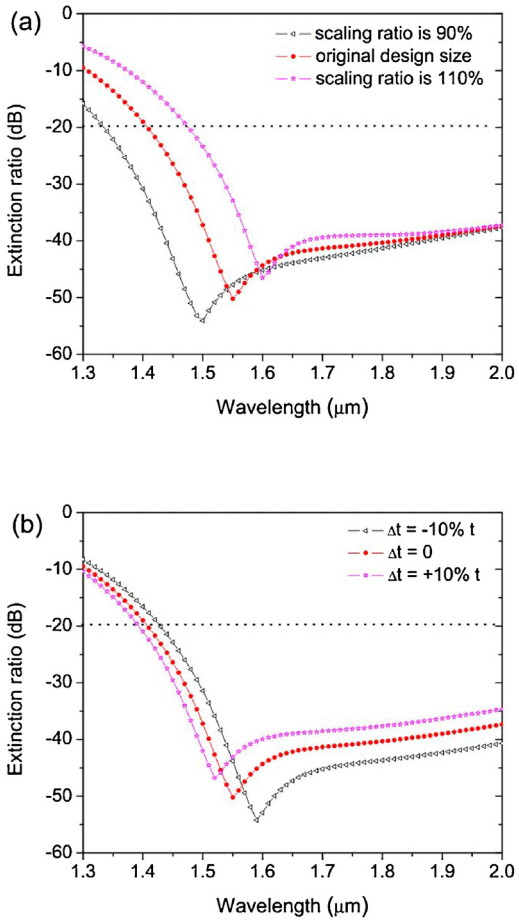

Fig. 8. Error tolerances of production are analyzed. (a) Error tolerances of the cross section. (b) Error tolerance of the thickness of the gold layer.

Compared with reference [16] and [17], our filter has the better filtering effect and the smaller insertion loss. The insertion loss of 0.07 dB is smallest as far as we know.

Acknowledgments

This project was supported by the National Natural Science Foundation of China (Grant No. 61475134 and 61505175) and the Science Research Projects of Hebei Province, China (Grant No. Z2017056, BJ2017108, 17210403 and 17210404).

References

[1] P.St.J. Russell, Photonic crystal fibers, J. Lightw. Technol. 24 (2006) 4729.
[2] D. Noordegraaf, L. Scolari, J. Lægsgaard, T.T. Alkeskjold, G. Tartarini, E. Borelli, P. Bassi, J. Li, S. Wu, Opt. Lett. 33 (2008) 986.
[3] H. Chen, S. Li, Z. Fan, G. An, J. Li, Y. Han, Photon. J. 6 (2014) 2201109.
[4] J. Guo, Y. Liu, Z. Wang, T. Han, W. Huang, M. Luo, Opt. Express 22 (2014) 7607.
[5] M.A. Schmidt, L.N. Prill Sempere, H.K. Tyagi, C.G. Poulton, P.St.J. Russell, Phys. Rev. B 77 (2008) 033417.
[6] X. Zhang, R. Wang, F.M. Cox, B.T. Kuhlmey, M.C.J. Large, Opt. Express 15 (2007) 16270.
[7] A. Nagasaki, K. Saitoh, M. Koshiba, Opt. Express 19 (2011) 3799.
[8] A.M. Heikal, F.F.K. Hussain, M.F.O. Hameed, S.S.A. Obayya, J. Lightw. Technol. 33 (2015) 2868.
[9] B. Sun, M. Chen, J. Zhou, Y. Zhang, Plasmonics 8 (2013) 1253.
[10] P. Li, J. Zhao, Opt. Express 21 (2013) 5232.
[11] A. Khaleque, E.G. Mironov, H.T. Hattori, Appl. Phys. B 121 (2015) 523.
[12] P. Geng, W. Zhang, S. Gao, S. Zhang, H. Zhang, J. Ruan, Photon. Technol. Lett. 24 (2012) 1304.
[13] A. Hassani, M. Skorobogatiy, JOSA. B 24 (2007) 1423.
[14] N. Florous, K. Saitoh, M. Koshiba, Opt. Express 13 (2005) 7365.
[15] H. Jiang, E. Wang, J. Zhang, L. Hu, Q. Mao, Q. Li, K. Xie, Opt. Express 22 (2014) 30461.
[16] C. Dou, X. Jing, S. Li, Q. Liu, J. Bian, Plasmonics 11 (2016) 1163.
[17] H. Li, S. Li, H. Chen, J. Li, G. An, J. Zi, Plasmonics 11 (2016) 1.